THE GELATION OF MONTMORILLONITE

PART 1.—THE FORMATION OF A STRUCTURAL FRAMEWORK IN SOLS OF WYOMING BENTONITE

By Marjorie B. M'Ewen and Margaret I. Pratt
Wheatstone Laboratory, King's College, University of London

Received 1*st August*, 1956

Light-scattering studies have been used to show that the basic structural unit in sols of Wyoming bentonite is a linear aggregate, one lattice layer thick, in which the particles are oriented edge-to-edge in the form of flat ribbons. In the presence of NaOH localized cross-linking of the ribbons, through edge-to-edge association, occurs but the formation of sheets or larger discs is not observed. No evidence for corrugated ribbons, formed by edge-to-surface interaction, or for micelle formation, due to surface association of the plates, has been found over the pH range 6·9 to 13. A three-dimensional structure, based on a system of cross-linked ribbons, which satisfies all the known experimental data is proposed.

Although it is generally accepted that the gelation of a lyophobic sol is due to the formation of an elastic framework, the nature of the interparticle forces responsible for its rigidity is still a matter of some dispute. According to the random-mesh theory of gel structure proposed for bentonite by Broughton and Squires [1] and modified by Goodeve [2] the particles are assumed to be in a brush-heap arrangement, bonded at points of contact by weak secondary forces. In the electrical, or long-range force, theory Heller *et al.*[3] postulate that the network is due to the association of aggregates which are composed of primary particles not in close touch but which assume equilibrium distances corresponding to positions of minimum energy. This hypothesis was based on the measurement of the sedimentation rate and light absorption in ferric hydroxide sols which indicated the growth of reversible aggregates; the magnitudes of the interparticle forces and distances were not, however, investigated.

The existence of long-range interparticle forces was established by the work of Bernal and Fankuchen [4] who observed the formation of non-equilibrium gels in suspensions of tobacco mosaic virus at concentrations above 1·8 %. Here the net interparticle forces are repulsive, presumably due to the interpenetration of their ionic atmospheres. At concentrations below 1·8 % the transformation to an equilibrium gel, in which the particles are separated by several hundred Ångstrom, is not easily explained since it seems unlikely that London-van der Waals attractive forces could be effective at such distances. The absence of birefringence in bentonite sols at rest [5] has been quoted as evidence against the existence of equilibrium attractive forces between the clay particles; this latter observation, however, is contrary to our findings described in the second part of this work.

The experimental evidence cited in favour of the random-mesh theory, such as the formation of gels in organic media and the simultaneous occurrence of gelation and electrical conductivity in mineral oils gelled by colloidal graphite,[6] seems to be strong for this type of system.

More recent advances in the theory of the forces between colloidal particles [7] have led us to carry out a systematic investigation of the optical and elastic properties of bentonite sols of known particle size, with the intention of putting the electrical theory to a quantitative test. Sols of Wyoming bentonite have been

chosen as a suitable system on account of their high colloidal stability and optical transparency.

The conception of a two-dimensional network in which the plates are aggregated edge-to-edge was first suggested by us some years ago.[8] Subsequently evidence in support of this model was obtained in the electron microscope.[9] It is, however, important to determine whether the aggregates seen in the electron microscope pre-exist in the suspension, since van Olphen [10] has suggested that in well-dialyzed sols structure formation is due to attractive forces between positively charged edges and negatively charged faces. The optical studies described in this paper have been designed to discriminate between the flat and corrugated ribbon models and to follow the growth of the structural framework under different conditions of pH. It then becomes possible to discuss the elastic properties, given in part 2, in terms of the magnitude of the interparticle forces within a framework of known form.

EXPERIMENTAL

Preparation of the sols

The sols were prepared from a 10% suspension of finely ground Wyoming bentonite in glass-distilled water (pH 6·5). After removal of the larger size particles by slow-speed centrifugation, the finer separation was effected by convective sedimentation[11] in a Sorvall angle centrifuge using a field of 20,000 *g*. After each run, of duration 20 min, the top straw-coloured layer was carefully removed and recentrifuged. Four or five spins of this type were sufficient to give a sol which subsequent experiments, described in this and in the following paper, showed to contain particles one unit lattice thick. Many of the physical properties described in this work appear to be peculiar to these completely dissociated layers. The concentrations of these sols, about 0·5% by weight, were determined by drying to constant weight at 108° C. More concentrated specimens used in the birefringence and elastic studies were prepared by slow evaporation *in vacuo*.

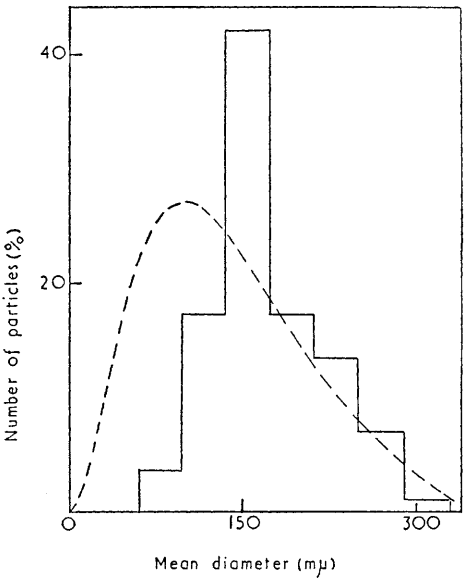

FIG. 2.—Particle size distribution in the electron microscope.

- - - particle size distribution deduced from light-scattering data.

Estimation of the particle size in the electron microscope

A gold-shadowed electron micrograph of the particles in an undialyzed sol is reproduced in fig. 1. The particles are thin polyhedral plates of mean diameter about 1500Å. Considerable overlapping occurs and it is not easy to distinguish the outlines of the individual particles; some of the larger units appear to be composed of smaller particles aggregated edge-to-edge. The particle size distribution, based on the measurement of 134 particles in six electron micrographs, is given in fig. 2, as it is of interest to compare these with the particle dimensions deduced from the light-scattering studies. It is difficult to describe the particle size by a single parameter and the mean diameter $\bar{d}$ is defined by the relation $\bar{d} = (2/\sqrt{\pi})\sqrt{\bar{a}\bar{b}}$, where $\bar{a}$ and $\bar{b}$ are the mean length and breadth measured in two directions at right-angles. It is thus the diameter of the disc whose area is approximately equal to that of the particle. Curling of the edges precludes estimation of the particle thickness by the shadowing technique.[10]

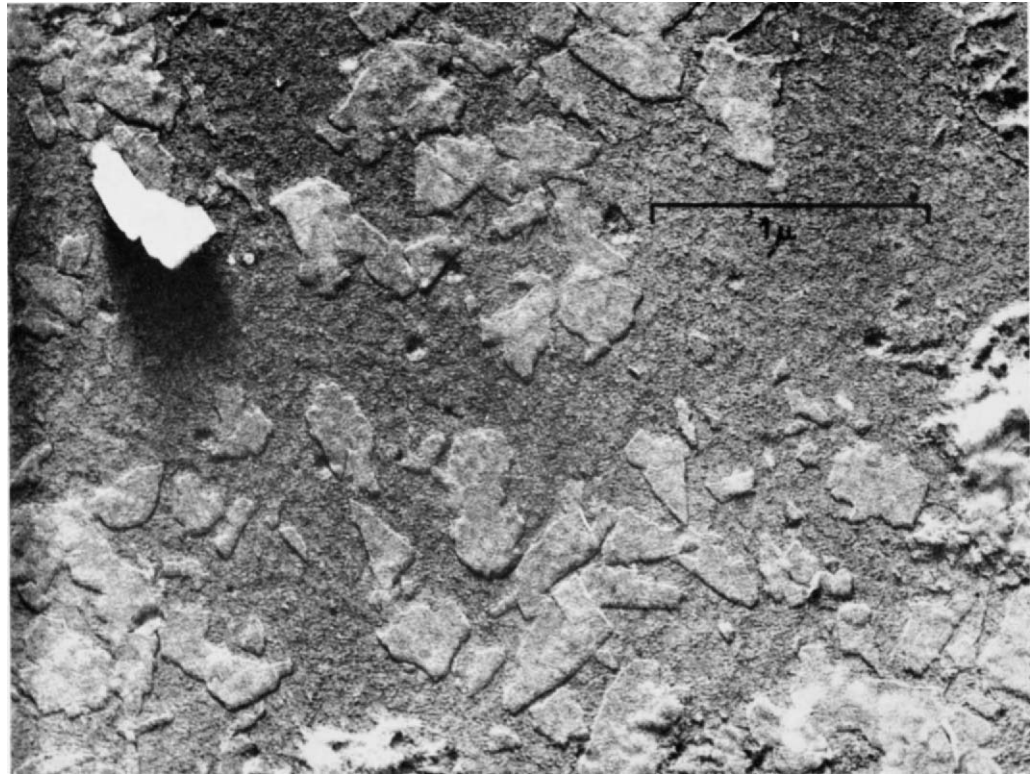

FIG. 1.—Gold-shadowed electron micrograph of the particles in an undialyzed sol.

[*To face page* 536

LIGHT SCATTERING MEASUREMENTS

The theoretical aspects and the experimental techniques of the light-scattering method in the study of macromolecules have been extensively described.[12] The method, which is based on the measurement of the reduced intensity of the scattered light (R) as a function of the scattering angle (θ), also affords a means of studying the shape and size of the aggregates in a colloidal suspension which is optically transparent. In the fundamental light scattering equation

$$\frac{Kc}{R} = \frac{1}{MP(\theta)} + 2Bc \qquad (1)$$

M is the particle weight (or for a polydisperse system, the weight average weight), K is a constant defined by $2\pi^2 n^2 \left(\frac{dn}{dc}\right)^2 \Big/ N\lambda_0^4$, n is the refractive index of the suspension, c is the concentration in g ml^{-1}, λ_0 is the wavelength *in vacuo*, N is Avogadro's constant and B is the interaction constant which characterizes the extent of the deviation from ideal solution behaviour. For *any* system of plates of uniform thickness, which is negligible compared with the wavelength, the particle scattering factor is given by an expression of the form,[13]

$$P(\theta) = (\pi/A\omega^2)F(b\omega), \qquad (2)$$

where A is the particle area, b is the particle breadth, $\omega = \frac{4\pi}{\lambda}\sin\frac{\theta}{2}$ and λ is the wavelength in solution. The functions $F(b\omega)$ for flat and corrugated ribbons, for polydisperse ribbons and for flat ribbons interacting edge-to-edge and edge-to-surface have been evaluated.* For monodisperse rectangular plates of side a and b,

$$F(b\omega) = \frac{ab\omega^2}{\pi}\sum_{s=0}^{s=n}\frac{(-1)^s\omega^{2s}}{(2s+1)!}\sum_{k=0}^{k=n}\frac{n!\,a^{2(n-k)}\,b^{2k}}{(n-k)!\,k!\,(2n-2k+1)(n-k+1)(2k+1)(k+1)}.$$

For $a > b$ the alternative expression,

$$F(b\omega) = \int_0^{b\omega} \Lambda_1(x)\,dx - \frac{2b}{\pi a}\left(\frac{\sin\frac{1}{2}b\omega}{\frac{1}{2}b\omega}\right)^2, \quad \text{where } \Lambda_1(x) = 2J_1(x)/x,$$

is valid for $a\omega > 6$ and more convenient than the series above. For long flat ribbons interacting edge-to-edge at an angle α,

$$F(b\omega) = \int_0^{b\omega} \Lambda_1(x)\,dx + f\cos b\omega\left(\frac{\sin\frac{1}{2}b\omega}{\frac{1}{2}b\omega}\right)^2, \quad \text{where } f = (2b/a)\operatorname{cosec}\alpha.$$

For long polydisperse ribbons whose breadth distribution is given by eqn. (5).

$$F(\bar{b}\omega) = \frac{2b_0\,\omega}{(1+b_0^2\omega^2)^{\frac{1}{2}}}\left\{1 + \frac{1}{2(1+b_0^2\omega^2)} + \frac{1}{2(1+b_0^2\omega^2)^2}\right\},$$

where $\bar{b}$ = mean ribbon breadth = $3b_0$.

For a system of corrugated ribbons composed of square plates of side b,

$$F(b\omega) = 4\sqrt{2}\,(b\omega)\int_0^1\int_0^1 (1-p)(1-q)J_0(v)\,dp\,dq,$$

where $v^2 = b^2\omega^2(p^2+q^2/2)$ and $J_0(v)$ is a Bessel function of zero order.

It is convenient for the interpretation of the experimental results to define a new function S by the relation $S = \left[\frac{R\sin^2(\theta/2)}{Kc}\right]_{c=0}$.

Eqn. (1) and (2) then lead to the result

$$S = (\rho\lambda^2/16\pi)\,F(\bar{b}\omega), \qquad (3)$$

where ρ is the molecular weight per unit area of the plates. Provided the plates are of uniform thickness, eqn. (3) holds for long polydisperse filaments if we insert the function $F(\bar{b}\omega)$ appropriate to the breadth distribution. For polydisperse systems characteristic oscillations in the functions $F(b\omega)$ are smoothed out and as $\bar{b}\omega \to 3{\cdot}8$, $F(\bar{b}\omega) \to 2{\cdot}0$. The function S thus approaches asymptotically to its limiting value

$$S_{\text{lim}} = \rho\lambda^2/8\pi. \qquad (4)$$

* We are indebted to Dr. A. R. Stokes for the following expressions.[13]

For a system of plates of mean breadth greater than $\lambda/3$ this limiting value will lie within the angular range of the photometer; the mass per unit area of the plates can then be determined. This is valuable information for long filaments with an axial ratio $m > 5$, where, on account of the rapid downward curvature in the $P^{-1}(\theta)$ plots as $\theta \to 0$, extrapolation of the Zimm plots to zero angle merely sets a lower limit to the particle weight. This is shown in fig. 5. Measurements at angles below 35° are very desirable but were precluded in our apparatus by the use of a light-scattering cell 40 mm wide, which was designed to avoid effects due to preferred orientation of the particles at the walls, birefringence studies having shown that this orientation may extend to a distance of 3 or 4 mm from the wall.

The design of the light-scattering photometer has already been described.[14] The constants of the apparatus have been redetermined by the turbidity method [15] using a

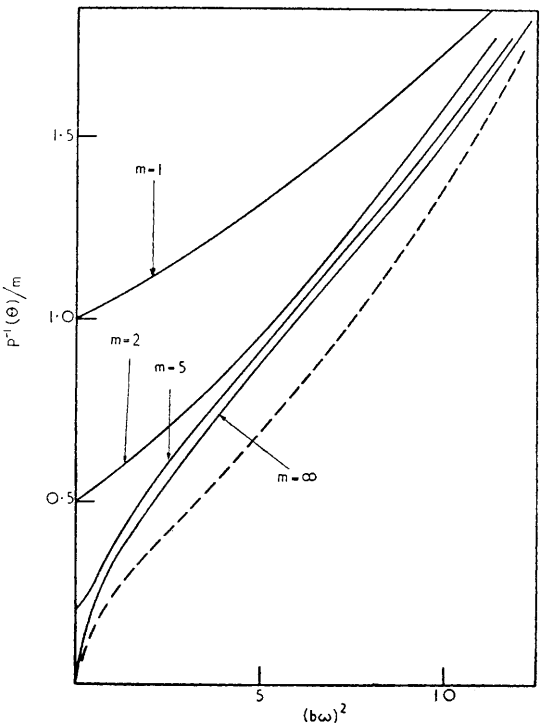

FIG. 3.—Theoretical reciprocal particle scattering factors for thin rectangular plates of side a and b showing the effect of increasing axial ratio $m = (a/b)$ on the form of the Zimm plot. The broken curve is the reciprocal particle scattering factor for a long corrugated ribbon formed by the edge-to-surface association of m square plates of side b, when $m \gg 1$.

sample of Ludox,[16] and the earlier calibration factors found to be correct to within a few per cent. Measurements were made using the wavelengths 5461 and 4539 Å; this not only serves as an experimental check but extends the values of ω covered by the angular range of the photometer. This is shown to advantage in fig. 9.

A sol, prepared as described above, was divided into two portions, one of which was brought to pH 6·9 by electrodialysis. The two specimens were then subjected to a further centrifugation at 20,000 g to free them of any optical impurities. Since both received the same centrifugal preparation comparison of the particle sizes can be made. Known weights of these clean stock suspensions were then added to optically clean water in the light-scattering cell, the pH of the water having been adjusted, if necessary by the addition of NaOH, to be equal to the pH of the stock suspension. The concentration of potential determining ions was thus the same in the light-scattering cell as in the prepared sol.

The background scatter from the water having been previously determined, a further correction to the observed intensities had to be made for the back reflection from the

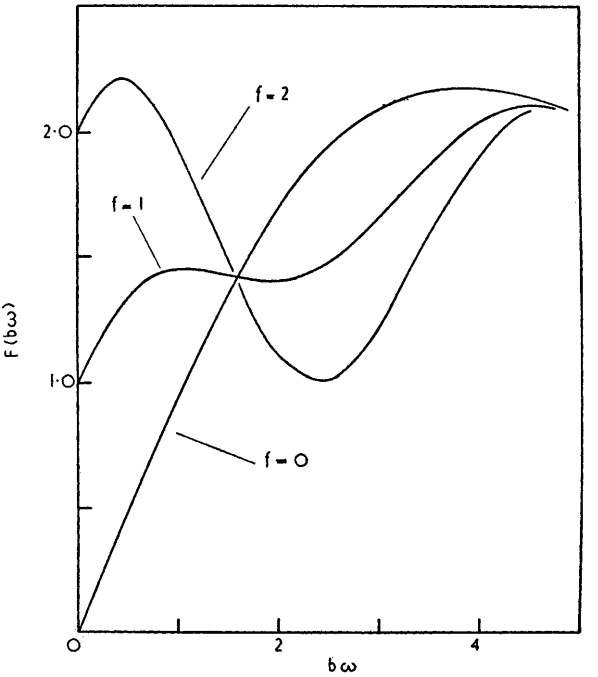

FIG. 4.—Showing the effect of edge-to-edge interaction on the function $F(b\omega)$ for long flat ribbons cross-linked at an angle α . $f = (2b/a)$ cosec α.

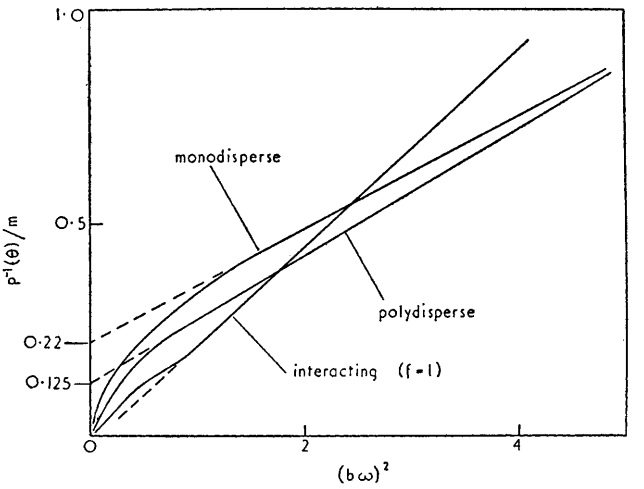

FIG. 5.—Showing the effect of polydispersity and edge-to-edge interactions on the low angle scattering in systems of long flat filaments.

exit window of the cell, on account of the high dissymmetry of the scattered light. This latter correction is negligible at angles below 50° but becomes increasingly important at higher angles.

RESULTS

Refractive index increment

Measurements of the refractive index increment of well-dialyzed sols were made against the dialysate in a differential refractometer. The instrument was calibrated with solutions of KCl using the data of Stamm.[17] The increment was found to be 0·095 ml g^{-1} independent of the wavelength over the range 5461 to 4359 Å.

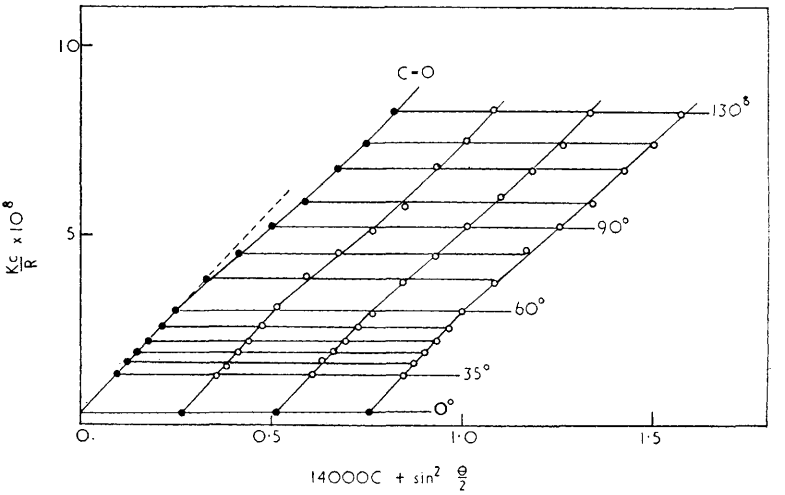

FIG. 6.—Zimm plot for undialyzed bentonite in water pH 8·9; concentrations: 1·87, 3·67 and 5·38 × 10^{-5} g ml^{-1}.

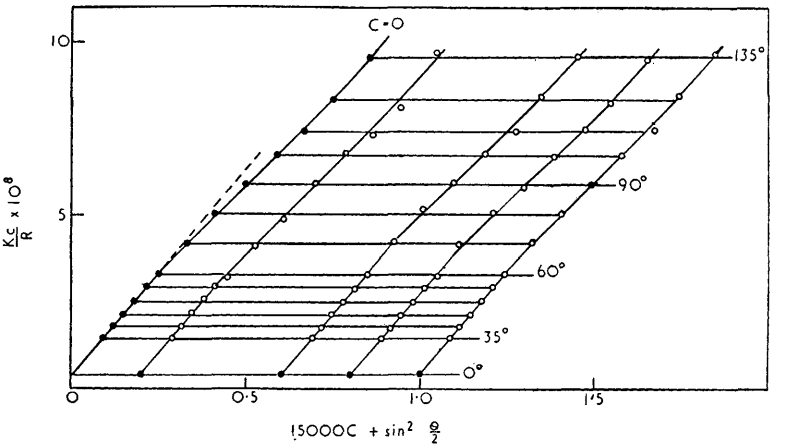

FIG. 7.—Zimm plot for electrodialyzed bentonite in water pH 6·9; concentrations: 1·32, 4·00, 5·34 and 6·34 × 10^{-5} g ml^{-1}.

Light scattering at low concentrations

Zimm plots for undialyzed bentonite in water at pH 8·9 and for electro-dialyzed bentonite in water at pH 6·9 are shown in fig. 6 and 7. Initially these plots are linear but at angles above 60° changes in curvature appear. This is typical of flat ribbons having an axial ratio m greater than 5, and in contrast to the gradual upward curvature characteristic of discs and corrugated ribbons as shown in fig. 3. Double extrapolation to zero angle and concentration indicates a weight average particle weight $\geqslant 2{\cdot}4 \times 10^8$ in the electrodialyzed sol and $\geqslant 4{\cdot}0 \times 10^8$ in the undialyzed sol. For reasons already

stated these can be regarded only as minimum values, and although we would like to establish a decrease in particle weight on electrodialysis we cannot treat these values as conclusive. For a system of ribbons with $m > 5$, the product $MP(\theta)$ at any given value of $\theta > 30°$ is a constant, and any increase in the length of the ribbons with increasing sol concentration will therefore not be detectable by the light scattering method. The lines of constant angle in the Zimm plots thus have zero slope.

ESTIMATION OF THE PARTICLE SHAPE AND SIZE IN THE ELECTRODIALYZED SOL.—The presence of ribbons has already been indicated by the oscillations in the Zimm plots in fig. 7 and the logarithmic plots in fig. 8 show that the experimental data for both wavelengths are best fitted to the theoretical curve for long, flat, non-interacting ribbons whose breadth distribution is given by

$$N(b)\mathrm{d}b = \frac{b^2}{2b_0^3} \exp(-b/b_0)\mathrm{d}b, \quad \text{with } \bar{b} = 3b_0. \tag{5}$$

From the displacement of the logarithmic scales in fig. 8 we find $\bar{b} = 1200$Å. This is the mean breadth of the system of long rectangular ribbons which give the same scattered

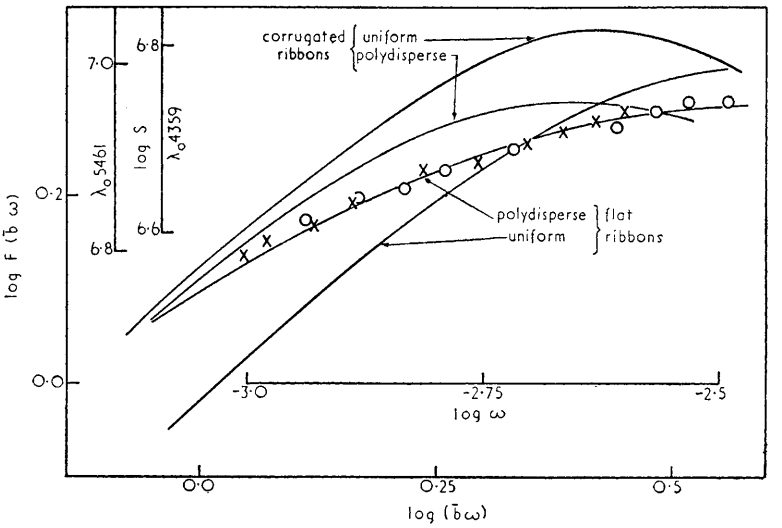

FIG. 8.—Logarithmic plots of $F(\bar{b}\omega)$ for flat and corrugated ribbons. Experimental values of log S for electrodialyzed bentonite in water pH 6·9, × for λ_0 5461 Å and ○ for λ_0 4539 Å.

intensity as a system of long filaments composed of irregular plates of mean diameter $\bar{d}$. Since the scattered intensity is always proportional to the surface area of the ribbons, $\bar{d}$ is to be identified with $(2/\pi^{\frac{1}{2}})\,\bar{b}$, and is thus found to be 1360Å. This is slightly below the electron microscope estimate of 1500Å ; the theoretical model, in which the variations in breadth within each ribbon are neglected, is, however, a poor approximation and better agreement is not to be expected. The particle size distribution, obtained by setting $b_0 = \bar{d}/3 = 45$ mμ in (5), is shown by the broken curve in fig. 2. This is a good fit with the size distribution in the electron microscope. The effect of the larger size particles is heavily weighted in the light-scattering method; differences between the theoretical and actual size distributions for the smallest sizes are therefore not detectable by this method. We thus have evidence that the scattering units in the dialyzed sol are *linear aggregates* in which the plates are oriented end-to-end.

Since this is the sol condition under which van Olphen [10] has suggested the attraction of positively charged edges to negatively charged surfaces it is important to consider further evidence against the corrugated ribbon model. If we identify the limiting value in the curve (*a*) in fig. 9 when $\omega = 3{\cdot}1 \times 10^{-3}$Å with the peak in the theoretical curve for corrugated ribbons at $\bar{b}\omega = 2{\cdot}6$, we find $\bar{b} = 840$ Å. Only 4 % of the particles seen in the electron microscope have small diameters of this magnitude. For flat ribbons, on the other hand, the S plots do not approach a maximum until $\bar{b}\omega = 3{\cdot}8$, and the mean

ribbon breadth calculated on this model is 1200 Å. We have not been able to compute the effect of a continuous distribution of particle sizes on the scattering from a system of corrugated ribbons; the theoretical curve in fig. 8 was therefore calculated for a hypothetical system in which 20, 45, 20 and 15 % of the particles have breadths b_0, $2b_0$, $3b_0$ and $4b_0$, with $\bar{b} = 2{\cdot}3b_0$. This is a very fair approximation to the actual size distribution in the electron microscope. No fit between the experimental points and any portion of this curve can be found. The corrugated ribbon model is thus not supported by the light scattering results. In part 2 we present birefringence and X-ray data which can only be interpreted in terms of an edge-to-edge interaction, and no evidence for the corrugated ribbon model has been found in any of this work.

Using eqn. (3) we deduce from the plots in fig. 8 that $\rho = 13{\cdot}6$ M.U./Å^2. The mass per unit area of the unit cell is accurately known from X-ray data to be 15·6 M.U./Å^2. Since isomorphous replacements within the lattice have little effect on the molecular weight of the unit cell, our estimate for the electrodialyzed sol is obviously low and we believe this may be due to our overestimating the concentration of the dialyzed stock

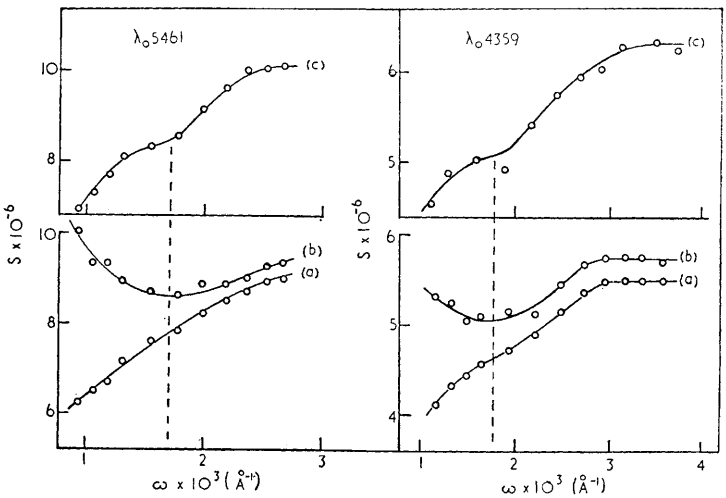

FIG. 9.—S plots (*a*) for electrodialyzed bentonite in water pH 6·9, (*b*) for electrodialyzed bentonite in 0·12 M NaOH, (*c*) for undialyzed bentonite in water pH 8·9.

suspension. The parent undialyzed sol, discussed below, for which an independent concentration measurement was made gives a value in exact agreement with the X-ray data. Hofmann and Bilke [18] have shown that water is more readily adsorbed on H- than on Na-montmorillonite; consequently it is possible that in drying to constant weight at 108° C we have failed to remove all the adsorbed water from the electrodialyzed bentonite although this temperature is sufficient to dehydrate the undialyzed material. The retention of six water molecules per unit cell is sufficient to account for an error of 15 % in the concentration and for the low value for ρ. Errors in the concentration do not affect the assessment of the particle dimensions.

The weight average particle area can now be estimated to be $\geqslant 2{\cdot}4 \times 10^8/13{\cdot}6$ Å^2 i.e. $\geqslant 1{\cdot}76 \times 10^7$ Å^2. (We correctly adhere to the experimental values, since concentration errors cancel out). The weight average area of the individual particles deduced from the electron microscope measurements is $3{\cdot}9 \times 10^6$ Å^2. The minimum number of particles in the ribbons in the electrodialyzed sol is thus about 5. We have investigated, as shown in fig. 5, the effect of polydispersity on the extrapolation of the Zimm plots to zero angle and find that for $m < 8$ the particle weight will be under- rather than over-estimated, while for $m = 8$ the extrapolation is exact. It thus appears that our estimate for the particle weight in the electrodialyzed sol may not be seriously in error and the evidence for a decrease in particle weight on electrodialysis is rather more convincing.

We now present quantitative evidence to show that in these sols edge-to-edge association of the particles to form sheets or larger discs does not occur. This is important because it is the configuration suggested by the electron micrographs and could be much more

readily explained. On substituting the limiting value of S attained by the curve (*a*) in fig. 9 into eqn. (4) we obtain a value for ρ *which is independent of the particle shape* and find $\rho = 13{\cdot}6$ M.U./Å^2. (The fact that we have already obtained this value by fitting the experimental points over the entire angular range to a theoretical curve for polydisperse ribbons is not the only evidence against the sheet model.) The weight average particle area of $1{\cdot}76 \times 10^7$ Å^2 corresponds to a disc of diameter 4700 Å. For such a system, the value of $b\bar{\omega}$ at 35° will be 5·4 and the function $F(\bar{b\omega})$ will already have attained its limiting value of 2·0. The S plots should therefore be lines of zero slope. This condition clearly does not occur in any of our sols.

EFFECT OF INCREASING pH ON THE PARTICLE INTERACTION.—Zimm plots for electrodialyzed bentonite in 0·12 M NaOH are not shown since the more subtle changes which take place with increasing pH are only revealed in the S plots given in fig. 9. For any given pH value the curves for the two wavelengths show characteristic features which occur at the same value of ω. They thus represent real effects in the sol and do not arise from any defect in the photometer at a particular scattering angle.

Except for a very slight inflection when $\omega = 1{\cdot}7 \times 10^{-3}$ Å the S plots for the sol at pH 6·9 indicate a system of non-interacting ribbons. On raising the pH this inflection becomes more pronounced and eventually changes to a minimum. The curves in fig. 9 bear a close resemblance to the theoretical curves for a system of long flat ribbons interacting edge-to-edge at an angle α (fig. 4). The curves (*c*) and (*b*) in fig. 9 approximate to the theoretical curves for $f = 1$ and $f = 2$ respectively. Since f is defined by $(2b/a)$ cosec α and b/a is $\ll 1$, the angle α must be small. This is the effect expected if localized cross-linking takes place through edge-to-edge interaction between two particles in adjacent ribbons. Exact parallelism of two ribbons does not occur, since there is no shift in the maxima of the S plots to lower values of ω. It is not clear whether this is due to the irregularity at the ribbon edges or to some property of the plates which limits the number of particles capable of cross-linking the ribbons, but the former seems the most likely hypothesis.

We have investigated the effect of polydispersity on the form of the theoretical curves for interacting ribbons and find that the function $F(\bar{b\omega})$ tends to a value which is less than 2·0 and which decreases with increasing interaction. Using the filament breadth distribution given by (5) we find for $f = 0$, $F(\bar{b\omega}) \to 2{\cdot}0$, for $f = 1$, $F(\bar{b\omega}) \to 1{\cdot}9$ and for $f = 2$, $F(\bar{b\omega}) \to 1{\cdot}8$. For the undialyzed sol for which f appears to be about unity we assume $F(\bar{b\omega}) \to 1{\cdot}9$. For λ_0 4359 Å the limiting value of S is $6{\cdot}3 \times 10^6$. Substitution of these values into eqn. (4) then gives the mass per unit area equal to 15·6 M.U./Å^2 in exact agreement with the X-ray value for the unit cell.

Over the pH range 6·9 to 13 the values of S_{lim} are constant within the limits of experimental error. Micelle formation due to parallel association of the basal surfaces does therefore not occur.

LIGHT SCATTERING AT HIGHER CONCENTRATIONS

At pH 6·9 these very dilute sols show no tendency to flocculate. This indicates that in the electrodialyzed sol the ribbons are colloidally stable; the absence of cross-linking has already been noted. At high pH values the sols, on standing for some hours, exhibit a slow reversible flocculation. Large flocs, visible to the eye in the light-scattering beam, settle under gravity at the bottom of the cell. Gentle magnetic stirring immediately disperses these flocs and restores the readings to their initial values. Measurements at higher sol concentrations were therefore made in an attempt to control the formation of these flocs and so investigate the possibility of some slower, secondary mode of particle association.

With increasing concentration the intensity of the scattered light is diminished more strongly at low than at high angles on account of external interference.[12a] These effects have to be taken into account in interpreting the measurements, which were restricted to the longer wavelength to reduce the effects of external interference to a minimum.

Fig. 10 shows the stable bottom layer ($c = 1{\cdot}73 \times 10^{-3}$ g ml^{-1}) which was formed overnight in the light scattering cell by the flocculation of a sol of electrodialyzed bentonite ($c = 0{\cdot}778 \times 10^{-3}$ g ml^{-1}) in 0·12 M NaOH. The scattering from the upper layer was indistinguishable from that of the suspension medium showing complete precipitation. Measurements on the bottom layer yielded the curve (*a*) in fig. 11. These measurements remained constant over a period of several days showing complete stability of the bottom

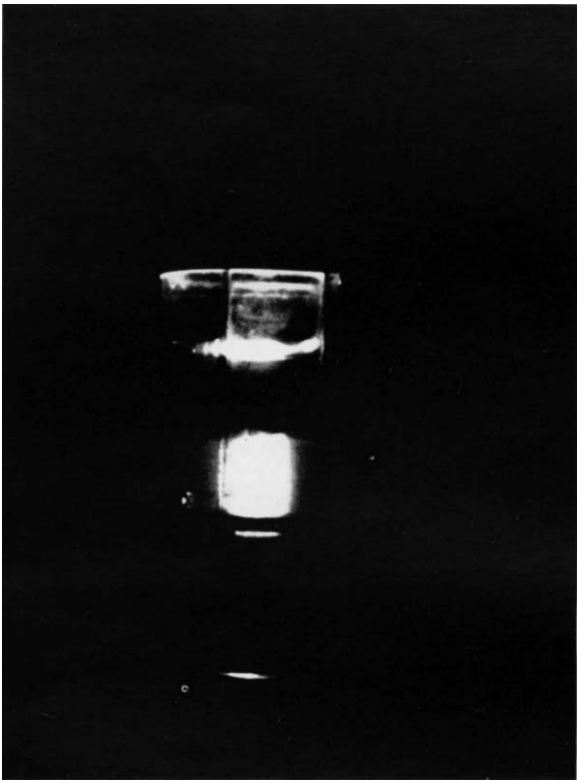

FIG. 10.—Showing the formation of a stable bottom layer ($c = 1{\cdot}73 \times 10^{-3}$ g ml^{-1}) formed by the flocculation of a sol of electrodialyzed bentonite ($c = 0{\cdot}778 \times 10^{-3}$ g ml^{-1}) in 0·12 M NaOH. A parallel light beam was passed vertically through the two layers which were photographed by scattered light.

[*To face page* 543

layer. The curve (*b*), which is shown for comparison, is for electrodialyzed bentonite in 0·12 M NaOH at infinite dilution. This curve was obtained by extrapolation of the Zimm plot to zero concentration and we note that it appears to extrapolate below the origin. This is in accordance with the conclusion, already drawn from the S plots in fig. 9, that in this sol the ribbons are interacting edge-to-edge at a small angle. The theoretical curve for such a system, which is given in fig. 5, shows that extrapolation from finite angles will indeed give a negative intercept unless values of $b\omega < 1$ can be brought within the angular range of the photometer. No changes, other than those due to external interference, are observed in the scattering from the bottom layer. At the higher scattering angles, where these effects are greatly diminished, the two curves closely approach, showing that the molecular weight per unit area of the scattering units remains unchanged. There is thus no evidence for micelle formation in the flocculated sol.

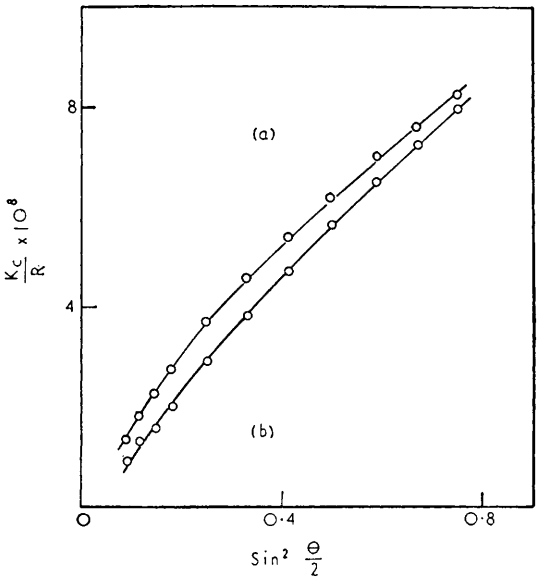

FIG. 11.—Reciprocal reduced intensity plots for (*a*) bottom layer and (*b*) sol at infinite dilution.

It is interesting to identify the concentration of the bottom layer with the concentration required to inhibit all rotation of the ribbons in one dimension, with consequent mechanical stabilization of the structure. By considering the volume available per ribbon it is easily shown that this will occur when

$$ac = 4\rho/\pi = 33, \qquad (6)$$

where a is the ribbon length in Å and c is the concentration in g ml^{-1}. For $c = 1{\cdot}73 \times 10^{-3}$ we find $a = 19{,}000$ Å. This corresponds to a ribbon with an axial ratio of 13, compared with the value of 5 found for low concentrations of electrodialyzed bentonite in water at pH 6·9, and is of a reasonable order of magnitude.

DISCUSSION

THE FORM OF THE STRUCTURAL FRAMEWORK

According to the random-mesh theory of gel structure, rigidity should appear simultaneously with mechanical interference between the particles. For the bentonite system this has been shown to occur when $c = 0{\cdot}17$ %, the concentration of the stable bottom layer. Using a very sensitive method, described in part 2, we have failed to detect *any continuous resistance to shear* at concentrations below 1 %. The random-mesh theory thus seems to be inadequate for the gelation of this system.

In fig. 12 we show a structure which conforms to all the evidence of the light-scattering studies and which utilizes the minimum amount of clay. We consider a small volume in the sol containing N ribbons (shown by the solid lines) which are linked at their ends at a small angle α, by edge-to-edge contact. The volume of the sol occupied by this structure is $Na^2b \sin \alpha$, and the volume available to N ribbons is $N\rho ab/c$. We therefore find the condition for continuity of structure to be

$$ac = \rho/\sin \alpha = 260, \quad (7)$$

where a is in Å, c is in g ml^{-1} and α is set equal to 0·1 in accordance with the light-scattering results. Comparison with eqn. (6) shows that the two theories of gel structure require concentrations differing by an order of magnitude. Although the structure leading to (7) conforms to all the experimental evidence, we do not suggest that this idealized arrangement, with its consequent regularities, will be observed in the sol; nor do we postulate that cross-linking will always take place at the ends of the ribbons, any of which can be extended as shown without violating the argument. The distance a in (7) must be regarded as the average distance between two consecutive cross-links on the same ribbon, while

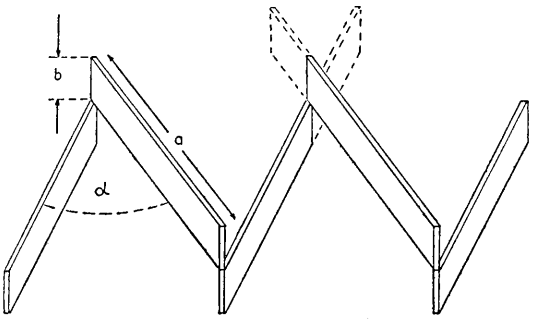

FIG. 12.—Proposed model of structure in sols of Wyoming bentonite. - - - extension of structure in three dimensions; $\alpha \sim 6°$.

the angle will be variable but always small. Inserting into (7) the value of a deduced from (6) we find for continuity of structure $c = 1{\cdot}3$ %. This is very close to the value found to be necessary for measurable rigidity. We thus have a model of a three-dimensional structure which appears to satisfy all the known experimental data. The tendency for the plates to form ribbons rather than sheets has yet to be explained.

CONDITIONS IN THE UNDIALYZED SOL AT pH 8·9

In water, exchangeable cations are desorbed from the lattice and form the counter ions of the electrical double layer. The pH rises due to partial hydrolysis with the formation of H-bentonite and free OH^- ions. The results given in this and in the subsequent paper can be accounted for if we make the reasonable assumption that in the undialyzed sol conditions at all the edges are not identical, i.e. the charge density and hence the double layer potential depends upon the direction of the edge in relation to the crystal axes.

The theoretical curves given in fig. 13 are based on the theory of Verwey and Overbeek [4] for flat plates whose approaching edges are large compared with the interparticle separation. For thin plates approaching end-to-end edge effects in one plane are neglected. This leads to values for the attractive and repulsive potentials *both* of which decrease too slowly with increasing particle separation. The form of the total potential energy curves is therefore not altered but the magnitudes given must be treated with considerable reserve. We have assumed for the London-van der Waals attraction constant (A) the value 2×10^{-12} erg.

This gives the best agreement with the experimental flocculation data for a number of sols,[7] and we find, as described in part 2, that this value fits well with the flocculation concentrations of univalent electrolytes for this sol.

Since the base exchange capacity of the bentonite is $\sim$ 100 mequiv. per 100 g of clay,[10] the concentration of the counter ions in a typical 0·5 % stock suspension will be $\sim$ 5 mequiv. litre^{-1}. The curve (*a*) in fig. 13 shows that at this concentration edges for which ψ_0 is less than 45 mV will show primary flocculation. The ζ-potential in an undialyzed sol deduced from measurements of the electrophoretic mobility is $-$ 40 mV; [19] the significance of this result in relation to the conditions at the edges is obscure and can only be regarded as indicating that the conditions predicted at the edges are of a reasonable order of magnitude. Below 50 mV the double-layer potential required for stability changes very rapidly with the concentration

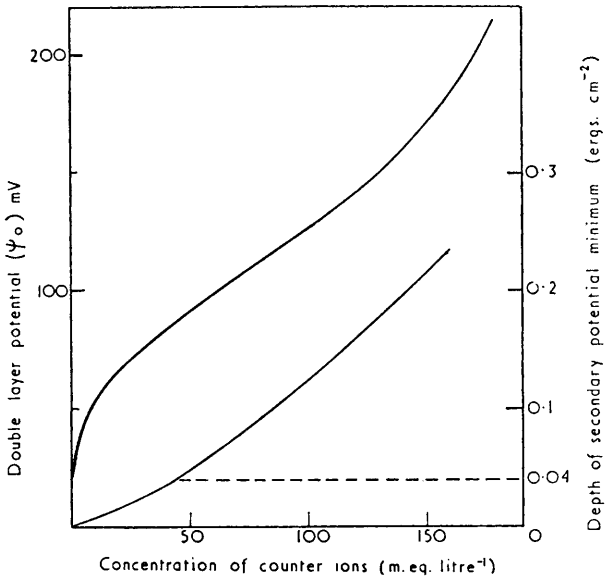

FIG. 13.—Theoretical stability curves for flat plates approaching edge-to-edge. (*a*) flocculating concentration of univalent counter ions as a function of the double-layer potential, (*b*) depth of secondary potential minimum as a function of the concentration of counter ions when $\psi_0 \geqslant 150$ mV.

of counter ions. Consequently quite small differences in the values of ψ_0 at the different edges would be sufficient to account for the formation of linear aggregates whose edges are colloidally stable. In the very dilute sols used in the optical measurements the concentration of potential-determining ions was the same as in the stock suspension and the concentration of counter ions was negligible. We can only conclude that under these conditions the primary aggregates formed in the stock suspensions are not repeptized in the light-scattering cell.

CONDITIONS IN THE ELECTRODIALYZED SOL

Electrodialysis stabilizes the sol by removal of the soluble electrolytes. The decrease of the double-layer charge by hydrolysis is at first relatively unimportant. This increase in stability is shown by the absence of cross-linking between the ribbons and by the absence of floc formation. Some indication of a decrease in the particle weight on dialysis has also been noted. Complete repeptization of the primary aggregates formed in the parent undialyzed sol does not, however, occur at pH 6·9.

EFFECT OF THE ADDITION OF NaOH

The sol is again stabilized, but by a different mechanism. The rapid increase in the particle charge is of primary importance. The ζ-potential rises rapidly to $-$ 70 mV and then becomes constant after the addition of about 25 mmoles NaOH litre^{-1}.[19] Further additions of alkali result only in compression of the electrical double layer. At high concentrations of counter ions the double layer potential may be several times the ζ-potential and values of $\sim$200 mV are quite possible. Pronounced cross-linking between the previously stable edges now occurs in the presence of 0·12 M NaOH. For this there appear to be two possible mechanisms. (1) Primary flocculation at edges for which ψ_0 is less than 140 mV. (It is difficult, however, to see why edges which were stable at pH 8·9 are not further stabilized by the increase in the particle charge.) (2) A loose secondary association of the edges in the shallow potential minimum which occurs at large particle separations. The depth of this minimum, read off the curve (*b*) in fig. 13, is 0·16 erg cm^{-2}; for plates of side 1300 $\times$ 10 Å this corresponds to an energy of $-$ 5 kT, which is more than sufficient to give a loose secondary association. The rapid dispersion of the flocs on gentle stirring is evidence in favour of this second hypothesis. The nature of the interparticle forces can only be properly investigated by measurements of the rigidity over a wide range of conditions as described in part 2.

The absence of micelle formation due to parallel association of the basal surfaces is readily explained. Because of the extreme thinness of the plates the attractive potential falls off much more rapidly in the parallel than in the edge-to-edge configuration. The repulsive potential, on the other hand, is independent of the configuration (edge effects being neglected). Consequently, except at very low values of the double-layer potential or very high concentrations of electrolyte repulsive forces predominate between the basal surfaces.

1 Broughton and Squires, *J. Physic. Chem.*, 1936, **40,** 1041.
2 Goodeve, *Trans. Faraday Soc.*, 1939, **35,** 342.
3 Heller, *J. Physic. Chem.*, 1941, **45,** 1203; Heller and Quimfe, *J. Physic. Chem.*, 1942, **46,** 765.
4 Bernal and Fankuchen, *J. Gen. Physiol.*, 1941, **25,** 111.
5 Hauser and le Bean, *J. Physic. Chem.*, 1938, **42,** 961.
6 McDowell and Usher, *Proc. Roy. Soc. A*, 1931, **131,** 409, 564.
7 Verwey and Overbeek, *Theory of the Stability of Lyophobic Colloids* (Elsevier Pub. Co., 1948).
8 M'Ewen and Mould, *Nature*, 1950, **166,** 437.
9 Mathieu-Sicaud, Mering and Perrin-Bonnet, *Bull. Soc. franc. min.*, 1951, **74,** 439.
10 van Olphen, *The Chemical Treatment of Drilling Fluids* (Thesis Univ. of Delft, 1951); also *Faraday Soc. Discussions*, 1951, **11,** 83.
11 Markham, *Faraday Soc. Discussions*, 1951, **11,** 223.
12 (*a*) Doty and Edsall, *Advances in Protein Chemistry*, 1951, **VI,** 35. (*b*) Zimm. *J. Chem. Physics*, 1948, **16,** 1093.
13 Stokes, *Proc. Physic. Soc.*, [in press].
14 M'Ewen and Pratt, *Nature and Structure of Collagen*, ed. Randall (Butterworths, 1953), p. 158.
15 Goring and Johnson, *Trans. Faraday Soc.*, 1952, **48,** 367.
16 Oster, *J. Polymer Sci.*, 1952, **9,** 525.
17 Stamm, *J. Opt. Soc. Amer.*, 1950, **40,** 788.
18 Hofmann and Bilke, *Kolloid Z.*, 1936, **77,** 239.
19 Mould, *Ph.D. Thesis* (Univ. of London, 1951).